



EVALUATING AND QUANTIFYING CASE STUDIES OF LIQUEFACTION-INDUCED FLOODING FROM CANTERBURY EARTHQUAKE SEQUENCE

C. Davis⁽¹⁾ and J. Hu⁽²⁾

⁽¹⁾ Waterworks Engineer, Los Angeles Department of Water and Power, Los Angeles, CA, Craig.Davis@ladwp.com

⁽²⁾ Civil Engineering Associate, Los Angeles Department of Water and Power, Los Angeles, CA, Jianping.Hu@ladwp.com

Abstract

Large areas in Christchurch, New Zealand and surrounding region were inundated multiple times as a result of earthquake-induced liquefaction initiated by the main events of the 2010-2011 Canterbury earthquake sequence. This study documents information collected for numerous flooded areas, including estimated flood depths where possible. The ejected water volume due to liquefaction is estimated for six cases from the post-earthquake topographic data. The volume change due to the liquefaction settlement is calculated from the ground surface pre- and post-earthquake digital elevation model based on LiDAR data. The estimated liquefaction induced settlement agrees very well with observed inundation depths, confirming expectations based on liquefaction being a constant volume process. In addition to liquefaction ejecta, there are other potential sources of the observed flood waters, including damage to potable, sanitary sewer, and storm drainage infrastructure allowing the water to leak onto the ground surface. In some locations these damaged infrastructures clearly contributed to the inundation, but evidence indicates these alternate sources provided relatively small volumes of the total documented flood waters. As a result, this study confirms the observed flooding resulted mainly from liquefaction ejecta. This finding is important because for the first time it documents the previously relatively unrecognized liquefaction-induced flooding hazard which needs to be considered in urban and land development planning.

Keywords: Liquefaction; Flooding; Canterbury Earthquake Sequence; Liquefaction-Induced Flooding; Case Studies

1. Introduction

Between Sept. 4, 2010 and Dec. 23, 2011, the Canterbury, NZ region was shaken by an earthquake sequence which caused a historically unprecedented amount of liquefaction-induced flooding in and around Christchurch. Many areas suffered severe liquefaction-induced flooding from multiple Canterbury earthquake sequence (CES) events. Although the water ejection process from liquefaction is well understood and manifested in laboratory testing, the extensive liquefaction-induced flooding from the CES provides a unique full-scale experiment to investigate this phenomenon. The CES provides numerous examples of liquefaction-induced inundation primarily from water and soil being ejected from the ground as a direct result of the liquefaction process. Documentation of the CES liquefaction-induced flooding and the resulting impacts to infrastructure are provided in [1] and [2]. This paper identifies specific case studies and performs initial evaluations of the liquefaction-induced flooding process. It also reviews in detail the potential water sources and shows the flooding is primarily from liquefaction.

2. Canterbury, New Zealand, Earthquake Sequence (CES) of 2010-2011

The Canterbury, New Zealand region was struck by a sequence of earthquakes in 2010 and 2011; the most significant being: M_w 7.1 on Sept. 4, 2010; M_w 6.2 on Feb. 22, 2011; M_w 5.8 and M_w 6.0 on June 13, 2011; and M_w 5.8 and M_w 5.9 on Dec. 23, 2011. The 2010 earthquake epicenter was located 45 km west of Christchurch while the 2011 earthquakes were about 6 to 10 km from the Christchurch city center. This earthquake sequence triggered soil liquefaction over wide areas for each main event [3]; the multiple earthquakes on June 13 and Dec. 23 are combined causal events. As shown in Fig. 1, the soil and water ejecta from the liquefaction process resulted in unprecedented surface flooding within minutes to hours after the shaking ended.



Fig. 1 – Liquefaction-induced flood in Christchurch City following the February 22, 2011 earthquake. (Crown Copyright 2011, NZ Defence Force – Some Rights Reserved)

3. Liquefaction-Induced Flooding

The earthquake-induced liquefaction process leading to flooding and sedimentation is described in [1] and [2], and is summarized herein with reference to Fig. 2. During earthquake shaking, the granular soil in Fig. 2 contracts, decreasing in volume. As the soil void space attempts to decrease, the load is transferred from the soil structure to the water mass, resulting in an increase in pore water pressure and stress reduction on the soil grains. When completely liquefied, soil particles are in a state of suspension and the water pressure equals the overburden pressure. As shown in Fig. 2, the excess water pressure is dissipated by upward water flow as the particles settle from their suspended state. The soil mass settles into a denser state. This is a constant volume process, which is indicated in Fig. 2 by showing the water ejected onto the ground surface remains at the same elevation as the original ground surface as the soil mass settles.

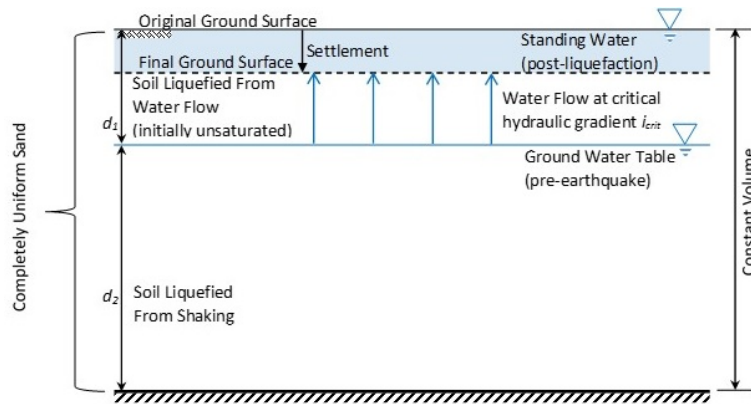


Fig. 2 – Uniform liquefiable sand deposit having pre-earthquake ground water table elevation at some depth d_1 below the original ground surface. The soils below hatched line are nonliquefiable; hatching is not an impermeable barrier. Water flow is unconstrained from sides and bottom.

Fig. 2 represents an ideal uniform soil condition having a horizontal groundwater and level ground surfaces. In reality soil deposits will contain less permeable layers (e.g., silt or clay) and/or more permeable zones (e.g., gravel pockets). These nonuniformities will change the water flow. Nonuniformities increase hydraulic gradients resulting in erosion of soil particles as explained in [1] and [2]. The subsurface water flow, erosion, and sedimentation onto ground has an analogy with common surface water flooding from rivers [1], [2]. The variation in permeability also changes subsurface water flow tending to focus ejecta through cracks, and potentially preventing ejection of material in some areas where pressure can dissipate in more permeable zones. Further, where there are slight changes in groundwater or land surfaces, the water will likely eject at the closest distance between the ground and water surfaces. For example, streets are commonly lower than adjacent properties; for horizontal groundwater surface and uniform soils, ejecta will first appear on the streets.

Because liquefaction is a constant volume process, as the ground settles the water and soil sedimentation deposition depth above the ground increases and inundates the surface as shown in Fig. 2. In the absence of surface drainage, the water surface elevation after the liquefaction process is completed remains approximately the same as the original pre-earthquake ground surface elevation. The variation in subsurface conditions and erosion process results in differential settlement across the ground surface. The inundation depth is approximately equal to the settlement when original groundwater is near the surface. This is the process causing the flooding in Fig. 1. The liquefaction-induced flood waters did not drain for many days [2] due to damage to the drainage system.

4. Evidence Supporting the Flooding is Primarily Liquefaction-Induced

There is a great amount of evidence supporting the premise post-earthquake surface water flooding was primarily from ground water ejected by the liquefaction process. However, because the liquefaction-induced flooding observed from the CES is not commonly associated with the general liquefaction phenomena observed in countless earthquakes around the world, there remains skepticism among some expert geotechnical engineers and geoscientists about the flood water sources exemplified in Fig. 1. This section provides observational evidence corroborating the liquefaction-induced flood hypothesis; the next section presents initial supportive evaluations.

Eye-witness accounts photographed and video recorded the water and sediment ejecting from the ground. Liquefaction-induced flood waters generally did not eject from the ground in large volumes during shaking, the mass ejection usually started several minutes after the earthquake shaking stopped. This ejection process was observed and documented by many people (e.g., <https://www.youtube.com/watch?v=TV7GTqU8YJ8>; <https://www.youtube.com/watch?v=2pzJS15u2PA>), and observed to last several hours [2].

Investigations were undertaken to identify the extent of liquefaction-induced flooding from the CES. Evidence was sought from printed literature and the World Wide Web; the results are summarized in [2]. The research confirmed 25 suburbs and portions of the Central Business District (26 total jurisdictional regions) experienced liquefaction-induced flooding in at least one of the four largest earthquake events in the CES. Seventeen suburbs were confirmed or expected to have flooded in at least three of the four events. Three of these suburbs were confirmed to have experienced flooding in all four main CES events. Flood areas are being distinguished here by entire jurisdictional suburb boundaries, however this does not mean the entire suburb flooded. In some cases, possibly only a few portions of streets located within the suburb flooded, but this is sufficient to identify the suburb as having experienced flooding.

Observations of post-earthquake flooding locations identify the inundation only occurred where moderate to significant liquefaction was experienced. Not all liquefied areas experienced flooding. There are no known locations of significant flooding in the Christchurch city region immediately following an earthquake in non-liquefied areas. These direct correlations between flooding and liquefaction serve as indicators the flooding resulted from the liquefaction process. However, liquefaction also has a significant impact on water infrastructure, which when damaged can provide sources for flood waters. As a result, further investigation of potential water sources is warranted.

The Avon, Halswell, Heathcote, Styx, and Wiamakariri Rivers flow through or in the vicinity of Christchurch city and are contained by levees (called stopbanks in New Zealand). However, no river overtopped its banks or flooded any lands at any time during the CES, even though stopbanks were damaged [4]. However, river water backflow from drainage pipes has been suggested as a possible flood contributor [3]. Fig. 1b shows the Avon River course with flooded streets and properties in the Bexley suburb. Some of the land in Fig. 1 is below the river level, making the backflow hypothesis [3] possible. However, many of the documented liquefaction-induced flooding locations occurred in areas far from rivers. Also, liquefaction-induced flooding occurred in many locations having elevations higher than the rivers (e.g., Dallington suburb). As a result, the rivers could not be the source of flooding, but backflow from drainage pipes may have contributed to inundation at some locations in some earthquakes.

Broken potable water, sanitary sewer, and storm drainage pipes are also possible sources of the flood water. Pipes can break from transient and permanent ground movements. Water flow from pipe breaks certainly contributed to flooding in some areas. However, video evidence (<https://www.youtube.com/>) shows the flooding process in many areas taking place as follows: (a) video does not show any pipe leakage existed from transient motions at end of shaking; (b) several minutes after shaking ended, small amounts of water began emerging from the ground; (c) as time progressed larger, and in some cases more violent, water and soil ejecta emerged from the ground looking like small linear fountains oriented along ground cracks which formed for several meters in length; (d) the volumes of ejected water and soil eventually flooded large areas. As previously identified, liquefaction-induced permanent ground movements did not occur until after earthquake shaking ended. In the absence of transient motions causing pipes to leak onto the surface, any water, sewer, or storm drainage pipe damages would have occurred when the ground spread laterally and settled differentially as a result of the ground water migration during the liquefaction process. Thus, significant pipe damages would not occur until after the ground water migration and ejection process was underway, which effectively prohibits the water pipelines from being the main initiator of the observed flooding. Pipe damage also exposes water as a point source, which was not observed in the videos documenting the flooding process. Further evidence comes from flooding in backyards contained by walls and fencing (e.g., https://www.youtube.com/watch?v=gDkLPLCC_Ok), open pastures, and park space where pipes do not exist and therefore could not contribute to the flooding; cases are presented in [2] where this is documented with photographic and video evidence. As a result, water, sewer, and storm drainage pipe breaks could not have caused flooding in all inundated locations, and as found in the next section, likely contributed relatively small portions of the total water volume in liquefaction-induced flooded areas.

Christchurch city receives all of its water supply from ground water wells. Some of these wells are artesian with pressure head several meters higher than ground level. Two artesian wells, one at the Bexley Pump Station (coordinates 43° 30' 40.34'', 172° 42' 54.41'') and one at Carters Road Pump Station (coordinates 43° 31' 15.37'', 172° 42' 20.79''), were damaged from liquefaction-induced ground movements in the February 22, 2011 earthquake [5]. The Bexley well flowed an estimated 150 m³/hour of water onto the ground surface for several days following the earthquake and added to the liquefaction-induced flood waters at the intersection of Pages Road and Anzac Drive, described later as Case A. The Carters Road well flowed lesser amounts and added to the liquefaction-induced flooding in Aranui in the vicinity of the area described later as Case C. These locations are observable in Google Earth satellite images taken on February 22 and 25, 2011 (GMT). The pump stations are flooded on the day after the earthquake. The artesian well water is observable in the Google Earth images on February 25, 2011 (GMT), but the amount of flow is insufficient to cause flooding and did not sustain the flood levels as the liquefaction-induced flood waters dissipated. Damaged wells with artesian flow were reported only for the February 22, 2011 earthquake. No documentation of damaged free-flowing artesian wells were identified for the other earthquakes as part of this investigation, although this may have occurred because many wells were damaged throughout the CES. As a result, well water did contribute to flood waters for at least two locations in one earthquake, but cannot be the primary source of flood waters in their areas or elsewhere in Christchurch city.

The above descriptions address all alternative possible sources of flood waters, including rivers, water pipes, sewer pipes, storm drainage pipes, and artesian wells. These potential sources individually or combined cannot be attributed to the flooding observed in all locations for all earthquakes. The only remaining potential source of water comes from the liquefaction process, which also is the only source having direct observable evidence for causing flooding. As a result, liquefaction is deduced to be the primary source of flooding, with some inundation locations having contributions from other sources, including artesian waters, which may have surfaced.

Liquefaction-induced flooding has rarely been reported (e.g. [6]) and is a previously relatively unrecognized hazard needing further investigation. Few, if any, studies have investigated liquefaction-induced flooding, but this hazard can have significant impacts on community resilience [1]. The CES highlights the rare but extreme inundation problems that can arise from liquefaction processes. Christchurch city also provides a unique opportunity to investigate and document numerous liquefaction inundation impacts on communities.

Such documentation is helpful to prepare for similar potential problems in other areas. The geotechnical and urbanized development conditions leading to such extenuating situations needs further investigation so guidelines for public policy and engineering mitigations can be developed and used worldwide. The next section presents initial investigations on liquefaction-induced flooding and sedimentation to move beyond observation, and better distinguish relative flood source contributions.

5. Evaluation of Liquefaction-Induced Flooding Using DEM and GIS

Liquefaction being a constant volume process provides the greatest supporting evidence linking the flooding to the ejecta and an opportunity for further investigation from documented observations. Large areas of the Canterbury Plain are relatively flat. Liquefaction of flat lands does not allow rapid drainage of the ejected water or experience large scale lateral spreading conditions. As a result, measured settlement of liquefied flat lands are mainly due to post-liquefaction reconsolidation and can be used to estimate the depths of ejected water and sediments. Important considerations included when developing an evaluation methodology are as follows:

- There are no direct measurements of flood levels in the CES, but numerous observations provide opportunity to estimate flood depths
- Photographic and video observations of liquefaction-induced flooding at known locations and approximate times provide useful case studies for research
- Post-liquefaction settlement at a point has uncertainty from the pre- and post-earthquake topographic data
- Uncertainty is expected to be reduced for cases where water volumes over known areas can be estimated. Water volumes can be estimated using Digital Elevation Models (DEM) derived from aerial Light Detection and Ranging (LiDAR) data.
- Settlement due to horizontal ground displacement, such as lateral spreading, is insignificant in study area

5.1 Identifying Liquefaction-Induced Flooding Cases for Study

Table 1 – Cases identified for studying liquefaction-induced flooding

Case	Event Date	Suburb	Location			Observed Inundation		Measured Settlement*
			Streets	Coordinates*		Object	Depth (cm)	
				Latitude (S)	Longitude (E)			
A	2/22/11	Bexley	Intersection Pages Rd. and Anzac Dr.	-43.510839°	172.715889°	Car bumper	20-30	10
B	2/22/11	CBD	Manchester St.	-43.525951°	172.639744°	Car tires	20-30	29
C	2/22/11	Aranui	Shortland St. at Rowses Rd.	-43.522125°	172.701614°	Car bumper	20-25	12
D	6/13/16	Aranui	Cuthberts Rd.	-43.523686°	172.706944°	Curb	10-15	6-8
E	6/13/16	Woolston	Ti Rakau Dr.	-43.552088°	172.695606°	Curb	20-25	20
F	6/13/11	Ferrymead	Ferry Rd.	-43.557569°	172.703128°	Truck tire	20-25	25

*Coordinates are for location of objects selected to estimate water depth. Settlement is measured using LiDAR at closest point to coordinates of object used in the evaluation and represents average settlement over 5 m x 5 m grid.



Fig. 3 – Locations of case studies, Christchurch city, NZ (Courtesy Google Earth)

As previously explained, research was undertaken to identify areas where liquefaction-induced flooding occurred from the CES main events. The research information was compiled to develop usable case studies. This effort initiated by looking only at areas where liquefaction was documented [3]. The research also investigated possible flooding outside of liquefied areas, and found none. Table 1 summarizes six cases from two CES events useful for presenting in this paper and Fig. 3 plots their locations. Of the hundreds of images documenting liquefaction-induced flooding for the CES, only those having identifiable location, earthquake, approximate time (i.e., date being same as earthquake), objects aiding in estimating flood depth, ability to estimate spatial coordinates, and available pre- and post-earthquake LiDAR measurements were used for this evaluation. There is sufficient information available to increase the number of case evaluations in the future.

5.2 Digital Elevation Models

The liquefaction-induced flooding is evaluated using the ground surface elevations derived from a suite of DEMs obtained from the Canterbury Geotechnical Database (<https://canterburygeotechnicaldatabase.projectorbit.com/>). These DEMs were derived from Aerial LiDAR surveys flown before, between, and after each of the major earthquakes. The LiDAR were acquired by AAM Brisbane (AAM) and New Zealand Aerial Mapping (NZAM). Table 2 presents LiDAR source and time of acquisition. The bare earth terrain models were created from LiDAR point clouds by removing points for structures and vegetation that were judged to be higher than 0.5 m above the surrounding ground [7]. The DEM was created from each terrain model by averaging the ground-return elevations within a 10 m radius of each grid point and represented in a 5 m grid.

Table 2 – LiDAR Source and Acquisition Time

Earthquake	Acquisition Date	LiDAR Source
Pre-Earthquake	July 6-9, 2003; July 21-24, 2005; Feb 6-11, 2008	AAM
September 2010	September 5, 2010	NZAM
Feb. 22, 2011	March 8-10, 2011 May 20-30, 2011	NZAM AAM
June 13, 2011	July 18 & 20, August 11, & 25-27, and Sep 2-3, 2011	NZAM
Dec. 23, 2011	Feb 17-18, 2012	NZAM

5.3 Elevation Accuracy

It is important to have high resolution and vertical accuracy topographic data in order to access the ground displacement due to liquefaction and associated flooding. Verification studies of LiDAR data are relatively few in comparison to the types of data utilization. Verification studies generally focus on elevation error for fixed lateral coordinates and utilize airborne LiDAR. As reported in the Canterbury Geotechnical Database [6], the NZAM LiDAR was acquired using instruments and procedures that give a fundamental vertical accuracy of 0.10 m (one sigma) for areas of open ground with hard surfaces. Metadata for the AAM LiDAR indicates a vertical

accuracy of 0.07 to 0.15 m, excluding GPS error and Geoid modelling error. Table 3 provides calibration statistics for the LiDAR point cloud sets. The 2003 and 2010 LiDAR have lower accuracy than the other post-earthquake sets resulting from less overlapping LiDAR swath. The vertical elevations were calibrated against land-based survey data supplied by the Christchurch City Council, Land Information New Zealand and Environment Canterbury from surveys of their benchmark networks [8].

Table 3 – LiDAR Source and Acquisition Time

LiDAR Source	July 6-9, 2003	Sept. 5, 2010	Mar. 8-10, 2011	May 20-30, 2011	July-Sept., 2011
Average error	-0.02 m	-0.04 m	0.03 m	0.01 m	0.05 m
Standard deviation	0.13 m	0.13 m	0.06 m	0.06 m	0.05 m

5.4 Methodology

The liquefaction-induced settlement is evaluated for areas with confirmed flood. The settlement was estimated using the pre- and post-earthquake DEMs. Google imagery, online photographs and videos were reviewed and analyzed to estimate the post-earthquake water depth at the time the images were taken. The evaluation is constrained to images available for review. Images used for case studies were selected based on them being taken within hours following the event. This is considered reasonable since the timeframe of a few hours between the event and photographic documentation is a small percentage of total flood drainage time, which took several days in many locations. The observed inundation depth presented in Table 1 is estimated based on scaling of identifiable objects in the photographs such as car tires, bumpers, curbs, etc. The coordinates of these objects are estimated by identifying approximate locations based on information observable in the photographs, mostly using Google Earth and Street View. There are inaccuracies inherent when estimating observed inundation depths from images; the observed inundation depths are therefore given as estimated ranges in Table 1.

A study area with fixed dimensions was determined based on observation of the flood area from field reconnaissance, Google imagery, and online photographs available after the events. The areal dimensions and location were selected to include and be representative of flooding observed around the identifiable objects selected from photographs (i.e., the study area bounds the object used to estimate water depth). The selected objects must be clear enough to provide reasonable estimation of the observed inundation depth. The settlement values in Table 1 were obtained from the difference between the pre- and post-earthquake DEM at the defined object locations. As mentioned above, the LiDAR DEM is developed in a 5 m grid with the vertical accuracy varying with mean from 1 cm to 5 cm and standard deviation from 5 cm to 13 cm. As a result, the estimated liquefaction-induced measured settlement value in Table 1 is that averaged over the 5 m grid in which the object coordinates are located. Settlement estimates made in this manner have an error related to the DEM processing procedure. This process error, combined with inaccuracies in estimating water depth and location from the photographic images, is attempted to be reduced by calculating the volume changes due to liquefaction using GIS surface analysis tools.

Table 4 presents results of the volume change estimates for each study area. The observed inundation volume for each study area is calculated using the observed inundation depth reported in Table 1 and the post-earthquake DEM. To make the observed volume calculation, a water surface is established by adding the observed inundation depth from Table 1 to the DEM elevation at the object coordinates. The observed inundation volume is calculated from the difference between a water surface elevation and the post-earthquake DEM and reported in relation to the observed inundation depth range. The settlement volume is the difference between the pre- and post-earthquake DEMs over the study area. Approximate trapezoidal study area dimensions are presented in Table 4.

Table 4 – Volume change estimates for study areas

Case	Event	Observed Inundation Depth	Measured Settlement (cm)	Estimated Settlement (cm)	Area	Study Area Volume Change (m ³)	
						Observed	Settlement

		(cm)				Inundation Volume	Volume
A	2/22/11	20-30	10	35-40	300m x 600m	16,720-26,020	33,440
B	2/22/11	20-30	29	35-40	130m x 160m	1,824-2,940	3,800
C	2/22/11	20-25	12	30-35	100m x 200m	1,059-1,408	2,420
D	6/13/16	10-15	6-8	10-15	60m x 110m	140-300	160
E	6/13/16	20-25	20	20-25	60m x 180m	300-470	370
F	6/13/16	20-25	25	20-25	50m x 100m	700-890	615

The areas evaluated have an average net settlement associated with the liquefaction solidification process. However, some areas have limited zones with a net uplift; it is unclear how much of the uplift zones are physically correct, but most are considered an artifact of errors from developing the DEM because the case study areas in Table 1 are, in general, not believed to be significantly affected by compressive uplift zones resulting from lateral spread or other means. Depending on the uplift or settlement, the displacement value will be either negative or positive. ArcGIS [9] surface volume tool is used to calculate the net settlement volume in the study area assuming zero as the reference plane. As illustrated in Fig. 4, the uplift volume is the cubic dimension between the reference plane and the surface above the plane and the settlement volume is the cubic dimension between the reference plane and the surface below the plane. The net volume change due to the displacement is the difference between the settlement volume and uplift volume for all calculations presented in this paper. Most study areas have negligible uplift. However, some uplift values may affect the final volume calculation; if these uplift values were identified as physically correct then they should not be subtracted from the settlement values because the vertical movements would displace water affecting the final flood depth. Further investigation is warranted for those uplift areas affecting final volume calculations.

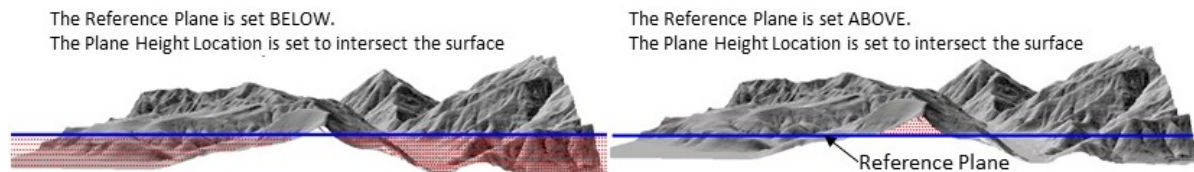


Fig. 4 – Settlement volume calculation using ArcGIS Surface Analysis Tool.

The estimated settlement in Table 4 is the range of water depths needed to bound the calculated settlement volume, assuming all settlement at the object location is derived from the liquefaction solidification process. The calculation is undertaken in the same manner as the observed inundation volume, except the observed water depth is not used. Instead a range of settlement values situated at the object coordinates are identified to calculate volumes within the study area bounding the settlement volume.

5.5 Liquefaction-induced Flooding Case Histories

5.5.1 Case A: Pages Road and Anzac Drive in Bexley Suburb, February 22, 2011

Fig. 5a is a Google Earth image the day after the earthquake (the image time is marked as 4PM 2/22/2011 GMT, NZ is 12 hours ahead) showing flood water remaining at the intersection of Pages Rd. and Anzac Dr. in the Bexley suburb of Christchurch city. Fig. 5b shows a vehicle driving north on Anzac Dr. The water depth is below the car bumper (the defined object in Table 1) and estimated to be about 20 to 30 cm. The exact N-S object location is difficult to identify within 5 m to 10 m from the Fig. 5b perspective. Fig. 5b is at mid-height of Fig. 1b, right side.



Fig. 5 – (a) Google Earth image intersection Pages Rd. and Anzac Dr. after February 22, 2011 earthquake in the eastern suburb of Bexley, dot locates object. (b) Flooding at the intersection (Courtesy T. O’Rourke)

The LiDAR data analysis indicates the measured settlement at this location is approximately 10 cm, however measured settlement in cells surrounding the object are between 17 cm to 30 cm. The study area is about 300 m x 600 m selected over the intersection. The settlement volume is 33,440 m³, and the potential flood volume ranges from 16,720 m³ to 26,020 m³, assuming 20 cm to 30 cm for the water depth at the car shown in Fig. 5b. The measured settlement agrees very well with the observed inundation depth in the area surrounding the object, but the settlement volume is larger than the observed inundation volume. The observed inundation depth is smaller than the estimated settlement, but within the range of measurement accuracy. The damaged artesian well at Bexley Pump Station contributed to flooding at this location. However, based on analysis results, the relative contribution from the well to overall flooding appears to be minor. This is reasonable considering the estimated 150 m³/hr flow within 6 hrs is 900 m³, which is small relative to that observed in Figs. 5b and 1b within this timeframe and the observed inundation and settlement volumes.

5.5.2 Case B: Manchester Street in the Central Business District, February 22, 2011

Fig. 6a shows a Google Earth image of the area covering the photograph in Fig. 6b about four days after the earthquake. Fig. 6b shows flooding of Manchester St. between Petersburg St. and Kilmore St. in the northern area of the Central Business District following the February 22, 2011 earthquake. The water was reported to be ankle deep liquefaction at Salisbury St. and south [10]. The depth is estimated to be about 20 to 30 cm based on depth of water at car tire in Fig. 6b and depth described as “ankle deep”. The object location is identified with high accuracy.



Fig. 6 – (a) Google Earth image covering locations in the northern area of the Central Business District following the February 22, 2011 earthquake, (b) Flooding at 250 Manchester St., between Petersburg and Kilmore Street looking east (Courtesy The Alfmeister, 2011).

The LiDAR data analysis indicates the measured settlement at the object location is approximately 29 cm. The study area is about 130 m x 160 m selected along Manchester St. between Kilmore and Petersburg Sts. The settlement volume is estimated to be about 3,800 m³. The observed inundation volume ranges from 1,824 m³ to 2,940 m³ for the observed inundation depths. Approximately 35 cm to 40 cm of water depth is needed to reach

the calculated settlement volume, which is reported in Table 4 as estimated settlement. The information used for this case is known to have been obtained before the ejection process was completed, so the observed inundation depth may have increased greater than seen in Fig. 6b. The observed inundation depth reported in Table 1 agrees very well with the measured settlement, but the settlement volume is higher than the observed inundation volume. The estimated settlement is larger than the observed inundation depth but is within the range of measurement accuracy.

5.5.3 Case C: Shortland Street and Rowses Road in Aranui Suburb, February 22, 2011

Fig. 7a shows a Google Earth image taken the day after the earthquake. This image shows large areas of liquefaction and remnant flooding. Fig. 7b shows a car driving south on Shortland St. The water at this location is estimated to be about 20 cm to 25 cm based on it reaching the front bumper. This is the defined object in Table 1, which is expected to be located with accuracy of 5 m in each direction. Estimating water and sediment depth for Fig. 7 is difficult because there is no observable reference to the street surface, so the observed inundation depth assumes there is no significant sedimentation on the street. The damaged artesian well at Carters Road Pump Station may have contributed to these flood waters, but is a relatively small influence just as found for Case A.



Fig. 7 – (a) Google Earth image taken four days after February 22, 2011 earthquake showing Case C and D study areas, dots locate objects. (b) Flood water at Rowses Rd. and Shortland St. (Courtesy M. Lincoln, nzraw.co.nz)

The LiDAR data analysis indicates the settlement at this location is approximately 12 cm, but the settlement in the adjacent grid is 15 cm. The study area is about 100 m x 200 m selected over the intersection. The settlement volume is 2,200 m³, but the observed inundation volume ranges from 1,059 m³ to 1,408 m³ for the range of observed inundation depths presented in Table 1. It would require about 30 cm to 35 cm of water at this location to reflect the settlement volume, as reported in Table 4 as estimated settlement. The observed inundation depth is higher than the measured settlement and lower than the estimated settlement, but within the measurement error.

5.5.4 Case D: Shortland Street in Aranui Suburb, June 13, 2011

Fig. 8a shows the location of Case D. This case is located just a little south east of Case C. Liquefaction damage in Aranui in the June 13, 2011 earthquakes was reported to be about as bad as from the February 22, 2011 earthquake [11] in this area. Fig. 8b shows flooding on Cuthberts Road in the Aranui suburb, located with relatively high accuracy. The inundation shown in Fig. 8a covered the street curb and sidewalk along the wall. The water depth is estimated to be about 10 cm to 15 cm based on standard curb height. Photographs of some surrounding streets taken about the same time indicate the flooding shown in Fig. 8b did not exist everywhere in the suburb.

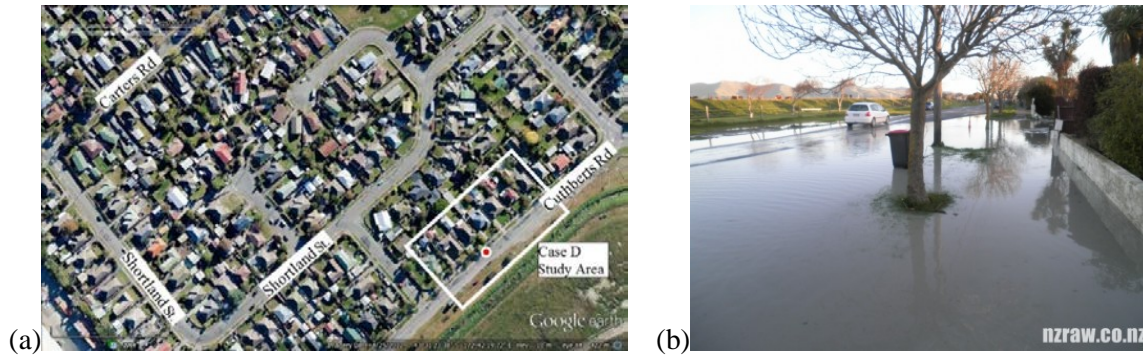


Fig. 8 – Cuthberts Rd. following the June 13, 2011 earthquake in the eastern suburb of Aranui. (a) Google Earth image 4/25/12. (b) Flooding on Cuthberts Rd., June 13, 2011 (Photo courtesy M. Lincoln).

The LiDAR data analysis indicates the settlement at this location is approximately 6 cm to 8 cm, depending on which portion of curb is selected. The study area is about 60 m x 110 m selected along Cuthberts Rd. The settlement volume is 160 m³, and the observed inundation volume range is around 140 m³ to 300 m³. The observed inundation depth and volume agree well with the measured settlement and the settlement volume, within the data accuracy range. The estimated settlement results match the observed inundation depth.

5.5.5 Case E: Ti Rakau Drive, Woolston Suburb, June 13, 2011

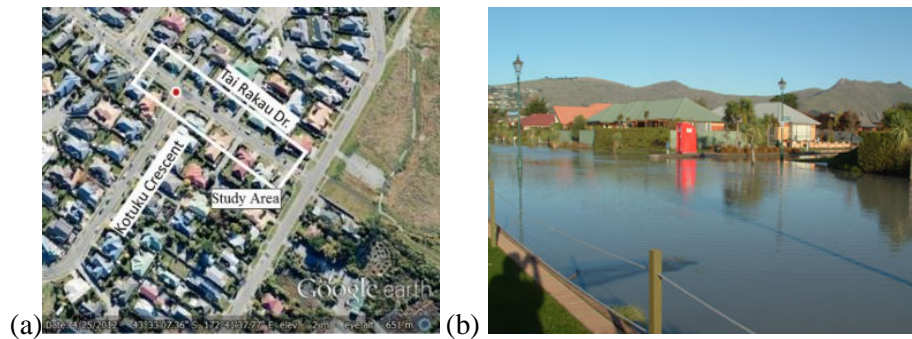


Fig. 9 – Ti Rakau Drive at intersection with Kotuku Crescent (a) Google Earth image after the June 13, 2011 earthquake in Woolston suburb, dot locates object. (b) Observed flooding (Courtesy of Brookhaven).

Fig. 9a shows a Google Earth image of Ti Rakau Drive in the Brookhaven neighborhood of the Woolston suburb in eastern Christchurch city. As shown in Figure 9b, the liquefaction-induced flooding is great enough to cover the street curbs and lawn. The observed inundation depth is about 20 cm to 25 cm based on curbs located with high accuracy. Drainage catch basins, observable in Google Street View, were unable to drain the flood waters.

The LiDAR data analysis indicates measured settlement at this location is approximately 20 cm. The study area is about 60 m x 180 m selected along Ti Rakau Dr. The settlement volume is 370 m³, and the inundation volume ranges from 300 m³ and 470 m³, for the range of estimated observed water depth. As seen in Table 4 for this case, the observed water depth, measured settlement, and expected settlement all agree very well. Additionally, the ground settlement volume agrees with the observed inundation volume.

5.5.6 Case F: Ferry Road in Ferrymead Suburb, June 13, 2011

Fig. 10 shows a Google Earth image of Ferry Rd. on February 25, 2011. This Case F is for the June 13, 2011 earthquake, but the image identifies areas where liquefaction ejecta arose from the previous CES earthquake. The photograph used to identify the object and location is seen at <http://www.gettyimages.com/detail/news-photo/vehicle-drives-through-water-on-ferry-road-near-sumner-news-photo/115959085>. The location is near 1013 Ferry Road, looking west, however there is difficulty in identifying the object location in the east-west direction due to the skewed distance perspective in the photograph. The photograph shows the water depth varies in this area. The observed inundation depth is estimated to be about 20 cm to 25 cm.



Fig. 10 – Google Earth image near 1013 Ferry Road dated February 25, 2011 in the eastern suburb of Ferrymead, dot locates object.

The LiDAR data analysis indicates the measured settlement at this location is approximately 25 cm. The study area is about 50 m x 100 m selected along Ferry Rd. The settlement volume is 615 m³, and the observed inundation volume ranges from 700 m³ to 890 m³. As seen in Table 4 for this case, the observed water depth, measured settlement, and expected settlement all agree very well. Additionally, the ground settlement volume agrees closely with the observed inundation volume.

5.6 Discussion

The evaluation results for these six cases shows how the measured inundation (water and sediment) matches closely to the ejecta, which is expected based on liquefaction being a constant volume process. Further, ejected inundation volumes are similar or less than the settlement volume, indicating external water sources likely played a lesser role in the flooding than the liquefaction ejecta. The results are remarkable considering the potential errors due to LiDAR data accuracy and location estimation. In general, the error for the liquefaction induced settlement (or settlement volume) is mainly from the LiDAR acquisition error and DEM interpolation, which is reported as 1 cm to 13 cm in 5 m grids. The error for the water volume is mainly coming from object location error and elevation error from LiDAR data. The evaluation process itself doesn't introduce any additional error.

There is also a high level of uncertainty in identifying some of the object locations and estimating inundation depths. These come from the lack of knowledge of when the images were taken verses the peak water height. The ejected water flows to lowest elevations, generally to street curbs, but the lower elevations are also generally the locations closest to the water table and where ejecta is produced. Water collected at lower elevations implies greater depth than what may have occurred. Lateral ground movements result in some vertical movement (settlement or uplift). Movable objects such as vehicles in the flood waters may rest on an unknown depth of sediment. Estimating the object location from single still photographs for some cases can be difficult. Lastly, some influx of external water sources and also drainage of the ejected water may respectively add and remove water affecting the estimated water depths; however, based on the evaluation results for all six case studies, external or alternate water sources seemed to have minor effect relative to large ejecta volumes for the CES flooded areas. There seems to be little effect from artesian water migrating to the surface independent of the liquefaction process.

The easiest way to compare evaluation results is by review of Table 4 columns three to five. Cases D, E, and F show these columns compare extremely well, tending to confirm the evaluation process and the inundation volumes being consistent with liquefaction theory. Cases A, B, and C have greater scatter. However, Cases A and B are found to be within the expected error and uncertainty, while Case C falls outside the uncertainty. Cases A, B, and C are from the February 22 earthquake and Cases D, E, and F are from the June 13 earthquake, indicating a possible seismic or data processing affect needing further investigation. Due to the large number of potential errors in the process, more case evaluations are warranted to ensure these initial results are statistically significant. Also, vertical movements resulting from potential lateral spread affecting case study sites needs further evaluation.

6. Conclusion

The liquefaction ejecta process during the Canterbury earthquake sequence (CES) was well documented and observable in social media posts (e.g., youtube.com and flickr.com), providing useful cases to study liquefaction-induced flooding. A detailed review of alternative water sources indicates the observed flooding was primarily from the liquefaction process. Six case studies were selected for initial evaluation. The results provide a very good correlation between observed flooding and that expected from the liquefaction ejection process, substantiating the hypothesis that the flooding was primarily from liquefaction. The initial studies presented herein identify the need to investigate additional cases. The CES highlights the rare but extreme inundation problems which can arise from the liquefaction process. Case studies as described herein are important to better understand the previously unrecognized liquefaction-induced flood hazard and develop ability to identify where this may occur elsewhere.

7. References

- [1] Davis, C. A., S. Giovinazzi, and D.E. Hart (2015): Liquefaction Induced Flooding in Christchurch, New Zealand. Proc. 6th International Conference on Earthquake Geotechnical Engineering, Nov. 1-4, 2015, Christchurch, New Zealand
 - [2] Infrastructure Resilience Division (IRD) (2017): Earthquake-Flood Multihazard Impacts to Lifeline Systems from the 2010-2011 Canterbury Earthquake Sequence. C. Davis, S. Giovinazzi, D. Hart, and A. Tang, eds., ASCE in development.
 - [3] Tonkin and Taylor (2012): Canterbury Earthquakes 2010 and 2011 Land Report as of February 29, 2012. Stage 3 Report, Prepared for the Earthquake Commission. <http://www.eqc.govt.nz/canterbury-earthquakes/land-claims/land-reports>.
 - [4] Green, R. A., A. Allen, L. Wotherspoon, M. Cubrinovski, B. Bradley, A. Bradshaw, B. Cox, and T. Algie (2014): Performance of Levees (Stopbanks) during the 4 September M_w 7.1 Darfield and 22 February 2011 M_w 6.2 Christchurch, New Zealand, Earthquakes. *Seismological Research Letters*, **82**, 939-949.
 - [5] Technical Council on Lifeline Earthquake Engineering (TCLEE) (2016): Christchurch, New Zealand Earthquake Sequence of M_w 7.1 September 04, 2010, M_w 6.3 February 22, 2011, M_w 6.0 June 13, 2011, M_w 5.9 December 23, 2011: Lifeline Performance. A. Tang, Ed., ASCE TCLEE Monograph, in press.
 - [6] Ishihara, K., Acacio, A. A. & Towhata, I. (1993). Liquefaction induced ground damage in Dagupan in the July 16, 1990 Luzon earthquake. *Soils and Found* 33, No. 1, 133–154.
 - [7] Canterbury Geotechnical Database (2015): Map Layer Descriptions. accessed 04/20/2016, <https://canterburygeotechnicaldatabase.projectorbit.com/>
 - [8] Canterbury Geotechnical Database Technical Specification 03 (2014): Verification of LiDAR acquired before and after the Canterbury Earthquake Sequence. <https://canterburygeotechnicaldatabase.projectorbit.com/>, accessed 04/20/2016.
 - [9] ESRI (2012) ArcGIS 10.3 for Desktop – Surface Volume, Copyright ©1999-2014 Esri Inc.
 - [10] The Alfmeister (Keith) (2011) Shake, Rattle and Roll...Pt III. posted February 22, 2011, <http://thealfmeister.wordpress.com/2011/02/22/shake-rattle-and-roll-pt-iii/>, Accessed December 28, 2014.
- Lincoln, M. (2011) June Earthquake 6.0 Photos. <http://www.nzraw.co.nz/news/june-earthquake-6-0-photos/>, posted June 13, 2011, accessed June 21, 2014.